Istraživanja i projektovanja za privredu
ISSN 1451-4117
DOI:10.5937/jaes0-42774
www.engineeringscience.rs

iipp publishing

Journal of Applied Engineering Science
Vol. 21, No. 3, 2023
Original Scientific Paper
Paper number: 21(2023)3, 1125, 837-845

SIMULATION OF THE DISTRIBUTION OF TEMPERATURE, STRESSES AND DEFORMATIONS DURING SPLINED SHAFTS HARDFACING

Oxana Nurzhanova[1], Olga Zharkevich[1*], Alexander Bessonov[1], Yelena Naboko[2], Gulnur Abdugaliyeva[1], Gulnara Taimanova[3], Tatyana Nikonova[1]

[1] *Department "Technological equipment, mechanical engineering and standardization", Faculty of Mechanical Engineering, Abylkas Saginov Karaganda Technical University, Kazakhstan*
[2] *Department "Nanotechnology and Metallurgy", Faculty of Mechanical Engineering, Abylkas Saginov Karaganda Technical University, Kazakhstan*
[3] *Department 'Thermal Physics and Technical Physics", Faculty of Physics and Technology, Al-Farabi Kazakh National University, Kazakhstan*

** zharkevich82@mail.ru*

This article describes the process of modeling the restoration operations of the destroyed segment of the spline and its complete restoration using modern methods, such as hardfacing in a protective gas environment with a consumable electrode. The ANSYS Workbench 19.2 software with an additional Welding Distortion and Moving Heat Source extension was used to simulate the process of hardfacing a damaged surface. The thermomechanical behavior of the deposited layer on the outer surface of the splined shaft is analysed. Dependences of the value of temperature fields on the parameters of the hardfacing mode in one and two passes depending on time are established. Dependences of residual stresses (0.413 - 239 MPa) and deformations (0.02 - 0.23 mm) in the process of semi-automatic hardfacing are determined. Experimental studies of samples during hardfacing were carried out for comparison with the geometry of the weld during modeling. The simulation results are in good agreement with the experimental data.

Keywords: hardfacing, temperature, stresses, deformation, spline

1 INTRODUCTION

To date, there are a huge number of methods for restoring worn surfaces of splined shafts of various techno-logical and economic indicators. The most common methods are manual arc hardfacing with stick electrodes, semi-automatic hardfacing using filler wire, and automatic hardfacing under a flux layer [1, 2, 3].

At Kazakhstani repair enterprises, semi-automatic hardsurfacing in shielding gases is most often used. This welding method is the most economical. It also provides good adhesion between the base and weld metal and has high productivity [4]. Semi-automatic hardfacing in a shielding gas environment allows you to perform restoration work in all spatial positions [5].

As a rule, shaft splines are welded with several welds [6]. The quality of the deposited weld depends on techno-logical parameters: amperage and arc voltage [7].

In order not to conduct expensive experiments to establish the optimal technological parameters of hardfacing, numerical modeling, and simulation using the finite element method are often used [8].

There are many papers on modeling welding and hardfacing processes. The papers [9, 10] describe the thermal deformation processes during welding, taking into account their non-stationarity and non-uniformity of thermal fields, as well as a numerical model that takes into account the most important welding input parameters (welding speed, current, voltage, and efficiency). The papers [11, 12] present modeling of multi-layer hardfacing with distribution of temperature, deformation and residual stresses of dissimilar welded butt joints with code written in ANSYS APDL and taking into account heat inputs in each element. The papers [13, 14] provide modeling of the restoration of hard-alloy surfacing parts. The results of numerical simulation revealed the trend of change and distribution of temperature fields and residual stresses during surfacing, taking into account the thermal cycle curve and phase transition effects. The conducted studies of existing methods for modeling the thermomechanical behavior of deposited layers do not take into account the possibility of joint use of ANSYS Workbench extensions with the birth and death technique to assess temperature distributions, strains and stresses.

Thus, in this work, the finite element method using the birth and death technique in ANSYS Workbench is used to determine the optimal hardfacing parameters, taking into account temperature distributions, deformations and stresses.

2 METHODOLOGY

In this work, to determine the residual stresses and strains, as well as the influence of temperature fields on the original part, a set of extensions for the ANSYS Workbench 19.2 software, such as Welding Distortion and Moving

Heat Source, was used. The selected extensions make it possible to recreate the hardfacing process with high accuracy and obtain reliable data.

The movable heat source used during hardfacing was calculated, models of damaged splined surfaces were created, and temperature fields were modeled. For the calculation, various values of the technological parameters of hardfacing were used and an analysis of residual stresses and deformations after surfacing was carried out. The result of this article is the choice of the optimal mode for surfacing a damaged section of splines, which provides the minimum allowable values of residual stresses and deformations of the part as a whole.

The construction of a finite element model was carried out according to the algorithm presented in Figure 1.

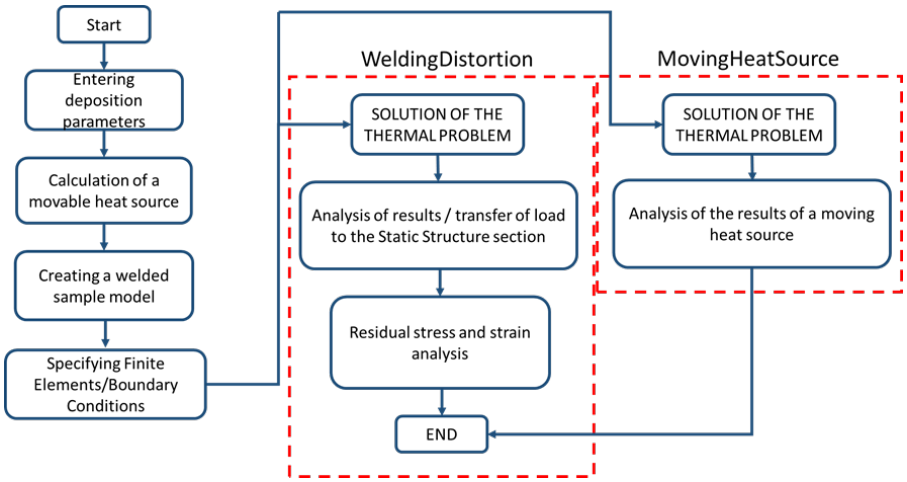

Fig. 1. Algorithm for constructing and solving the problem of modeling the surfacing process

To build a moving heat source when simulating the hardfacing process using the Moving Heat Source extension, an expression for non-stationary heat transfer in three-dimensional space was used. This expression has the following form [16]:

$$\frac{\partial}{\partial x}\left(k\frac{\partial T}{\partial x}\right)+\frac{\partial}{\partial y}\left(k\frac{\partial T}{\partial y}\right)+\frac{\partial}{\partial z}\left(k\frac{\partial T}{\partial z}\right)+\dot{Q}=\rho C_p\frac{\partial T}{\partial t} \quad (1)$$

where ρ – material density;
k – thermal conductivity of the material;
C_p - specific heat capacity of the material of the workpiece or part;
t - hardfacing time;
T – hardfacing temperature;
Q – the energy value of the moving heat source (welding arc).

The boundary condition for the heat transfer phenomenon takes the following form [17]:

$$k_n\frac{\Delta T}{\Delta x}-q+h(\mathrm{T}-T_0)+\sigma\varepsilon(T^4-T_0^4)=0 \quad (2)$$

where k_n - thermal conductivity of the material;
h - heat transfer coefficient (the transfer of heat from gas to gas during forced movement is taken as the heat transfer coefficient equal to 10 W/m^{2}K);
ε - emissivity;
σ - Stefan-Boltzmann constant;
T_0 - ambient temperature;
ΔT – temperature gradient;
Δx - the size of the heat source along the x-axis.

The value of the moving heat source is determined according to the formula (3) [18]:

$$\dot{Q}=\frac{6\sqrt{3}f_i p\eta}{\pi\sqrt{\pi}abc}\exp\left(-\frac{3x^2}{a^2}-\frac{3y^2}{b^2}-\frac{3z^2}{c^2}\right) \quad (3)$$

where p – heat source power (welding arc);
η – thermal efficiency of the arc or effective efficiency of the product heating process, taken equal to η = 0.8, taking into account gas-shielded welding with a consumable electrode and jet transfer of molten filler metal;
a, b, c – semiaxes of a double ellipsoidal heat source;
f_i – dimensions of the thermal field of the heat source.

The object for simulating the hardfacing process was a splined shaft (Figure 2). The overall dimensions of the part are equal: length - 100 mm, diameter along the tops of the slots - 55 mm, diameter along the hollows of the slots - 50 mm, width of the spline - 8 mm.

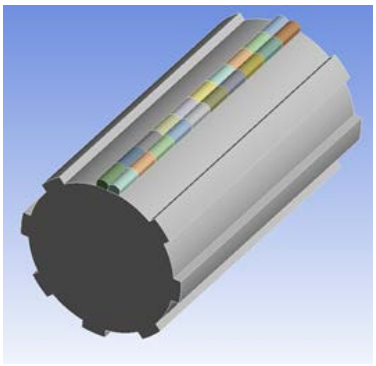

Fig. 2. Model of the restored spline by semi-automatic hardfacing

Structural steel 45 according to GOST 1050-2013 is used as the main material of the destroyed spline shaft. The chemical composition of the presented steel is shown in Table 1.

Table 1. Chemical composition of structural steel 45

Material	C	Si	Mn	Ni	S	P	Cr	Cu
Steel 45	0.42-0.50	0.17-0.37	0.50-0.80	≤ 0.3	≤ 0.035	≤ 0.030	≤ 0.25	≤ 0.3

For experimental hardfacing, a semiautomatic device PDG-252 (SELMA, Ukraine) with a built-in wire feed mechanism and a universal welding carriage with magnetic clamps was used. Hardfacing was carried out in a shielding gas environment. The equipment used was provided by the laboratory of the Kazakhstan Institute of Welding at the Abylkas Saginov Karaganda Technical University. Hardfacing modes were selected empirically. The main requirement for the weld was to obtain the highest height of the deposited layer while ensuring the fusion of the deposited metal with the test sample.

To simulate the hardfacing process, the technological parameters of the regimes indicated in Table 2 were used.

Table 2. Parameters of the splined shaft hardacing mode

Mode	Amperage, A	Voltage, V
1	135	20
2	180	19,5
3	220	20
4	240	22
5	260	22

The effective thermal power is determined by the formula [15]:

$$Q=U*I*\eta \quad (4)$$

where U – arc voltage;

I – amperage;

η - thermal efficiency of the arc.

Taking into account the hardfacing mode parameters (table 2), the value of the movable heat source was calculated according to formula (3) and the effective thermal power according to formula 4. The data obtained are presented in table 3.

Table 3. The value of the movable heat source

Mode	Amperage, A	Voltage, V	Effective thermal power, J/s	The value of the moving heat source, W/mm^3
1	135	20	2160	25
2	180	19,5	2808	26
3	220	20	3520	28

4	240	22	4224	30
5	260	22	4576	33

Creating a model of a welded seam on a damaged surface of a splined shaft includes such operations as: pre-processes, calculation, post-processes (Figure 3).

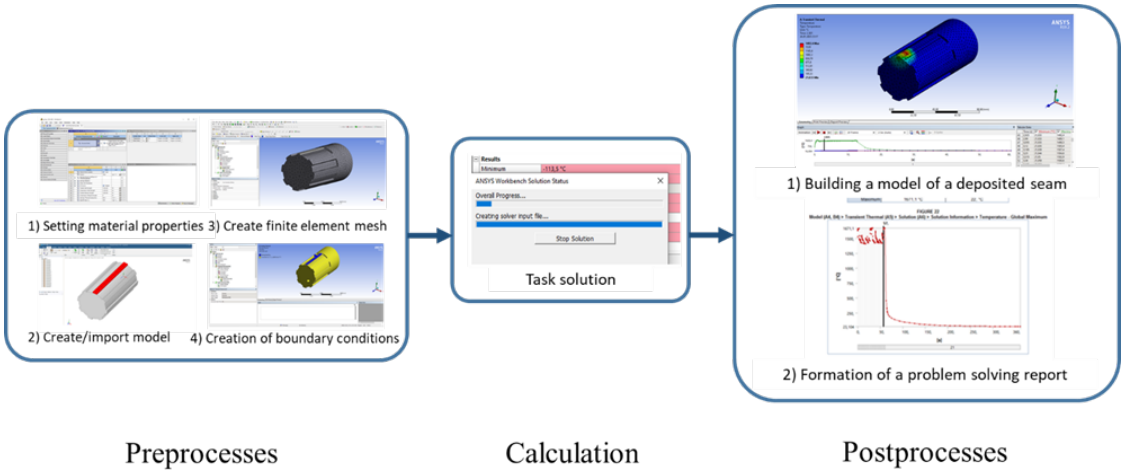

Fig. 3. Stages of creating a spline recovery model

3 RESULTS AND DISCUSSION

The results of hardfacing modeling in the first mode of Table 3 are presented in Figure 4. The results are considered depending on the time of passage of the welding arc in a certain section of the spline.

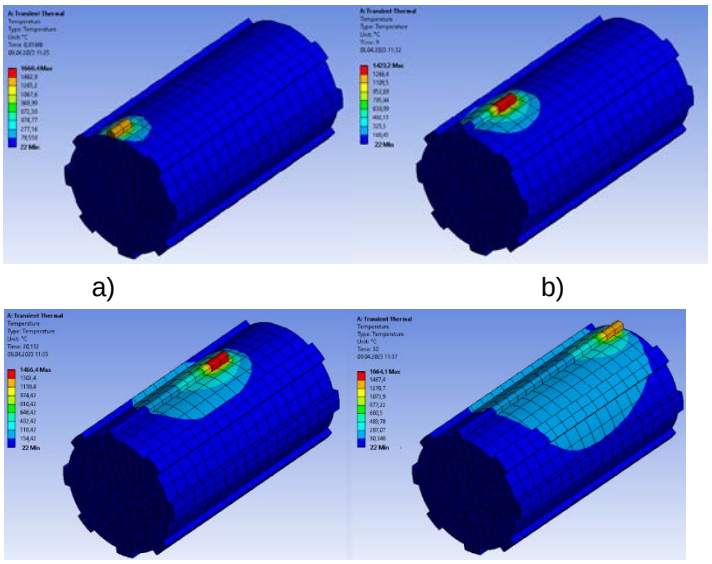

Fig. 4. Change in temperature fields during the first pass: a) temperature after 1 second, b) temperature after 5 seconds, c) temperature after 9 seconds, d) temperature after 20 seconds

It should be taken into account that the error of the result is associated with the increased length of the weld segment, which is necessary to reduce the complexity of the calculation processes.

As can be seen from Figure 4, the maximum temperature of the deposited weld is 1661°C, which corresponds to the melting temperature of the selected material. When modeling the hardfacing process, the influence of the welding arc temperature on the surface of the part to be restored is excluded.

Analyzing the obtained temperature fields, it was found that in the first 3 seconds (Fig. 4, a) of the hardfacing, the largest diameter of the temperature effect is approximately 30 mm, where the surface temperature of the part reaches T = 283°C. During further surfacing, newly applied weld segments prevent complete cooling of the part surface and, as a result, after 20 seconds, i.e. the passage of the heat source of the entire length of the part, the temperature field T = 325.3 ° C covers an area equal to ~ 1500 mm^2.

According to the specified parameters of the part and the width of the original slot, in order to obtain a rough shape of the restored surface, it was necessary to perform multilayer surfacing.

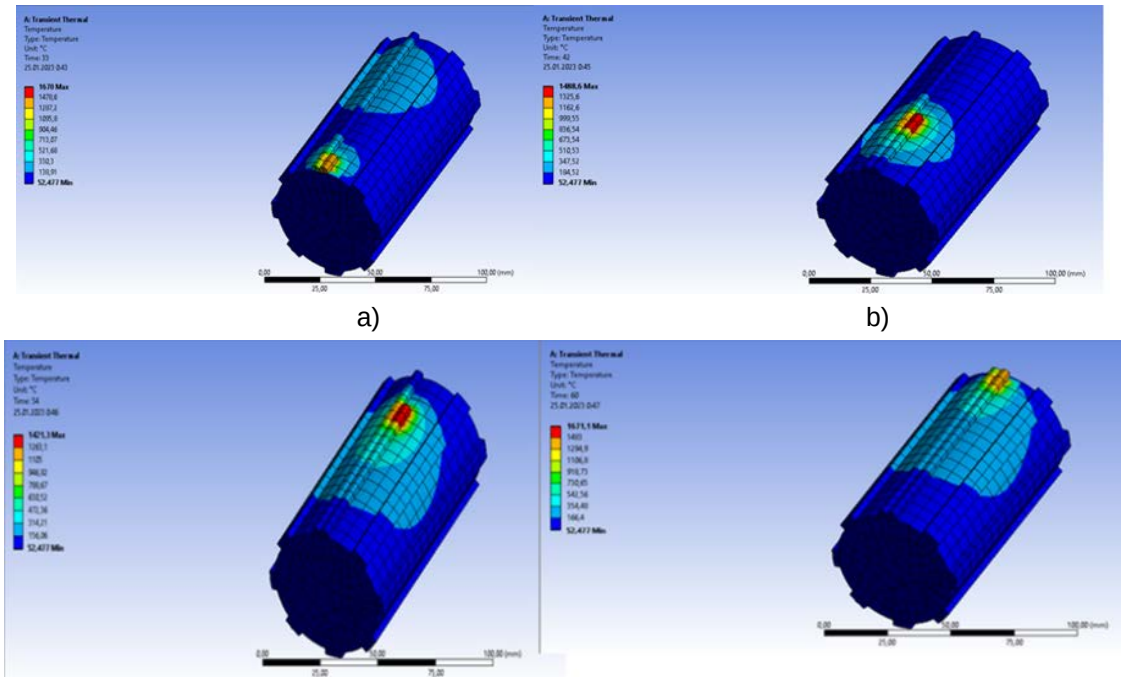

a) b)

c) d)

Fig. 5. Change in temperature fields during the second pass: a) temperature after 21 seconds, b) temperature after 28 seconds, c) temperature after 35 seconds, d) temperature after 40 seconds

After analyzing the results obtained in Figure 5, one should notice a trend towards an increase in the area of zones with a temperature of T = 166 to 710 °C, marked with a gradient from blue to green, which is the result of sequential, multilayer hardfacing. The lack of time to reduce the temperature of the original part contributed to an increase in the area of the temperature field T = 166°C, thereby covering more than 15% of the restored part, which increases the likelihood of developing residual deformations.

When performing multi-pass hardfacing of a damaged surface, excluding the cooling time of the part, there is an increase in the tendency for the formation of residual deformations due to an increase in the temperature of the part.

The results obtained contribute to further analysis of the influence of the parameters of surfacing modes on the change in temperature fields and the magnitude of residual temperatures, the duration of cooling of the part to the standard ambient temperature (22°C).

Figure 6 shows samples with a multi-layer hardfacing of a destroyed spline after 194 seconds from the start of hardfacing.

It follows from Figure 6 that when changing the mode parameters, not only the area of the considered temperature fields changes, but also the temperature of the part in the measured time interval (after 194 seconds from the start of surfacing or after 134 seconds from the start of cooling of the part). So, when using the 1st mode parameters (table 3), the temperature of the restored part after 194 seconds drops to T = 95.326°C. During the same period of time, when using the 3rd mode parameters (table 3), the temperature of the restored part reaches 125.85°C. The difference in the residual temperature of the restored part at the same time interval is justified by the change in the used parameters of the surfacing mode.

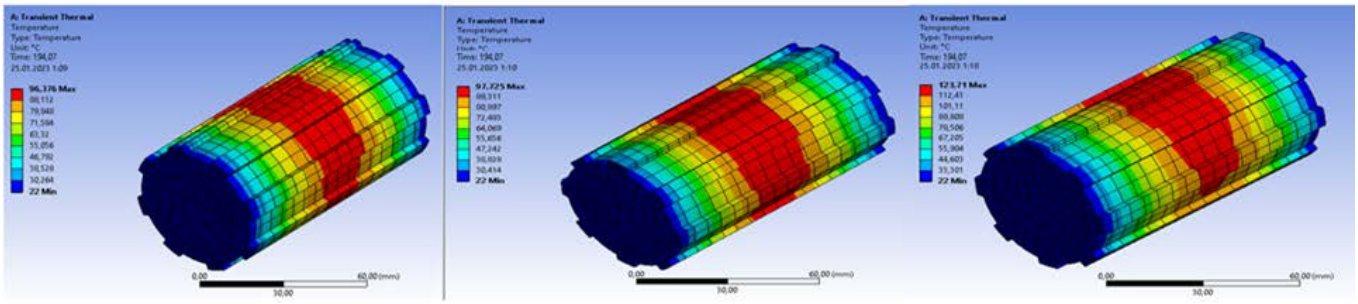

a) b) c)

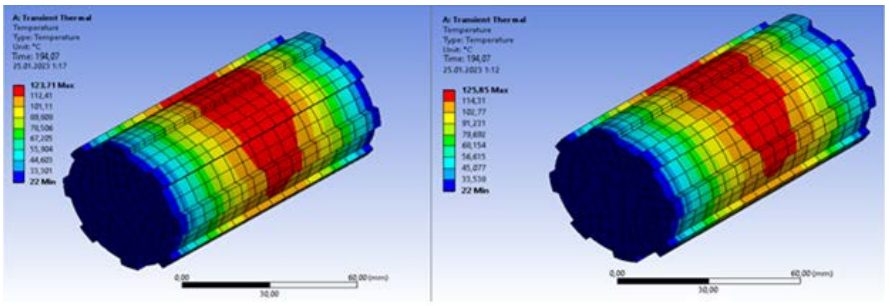

d) e)

Fig. 6. The value of the residual temperature after 194 seconds from the start of hardfacing: a) I=135A, U=20V; b) I=180A, U=19,5V; c) I=220A; U=20V; d) I=240A, U=22V; e) I=260A, U=22V

Complete cooling after multi-pass surfacing in modes 1-5 (Table 2) is achieved in about 290-310 seconds after the start of hardfacing. In the further calculation of the problem, no changes in the temperature of the part were observed.

The temperature values for various hardfacing modes and the part cooling are presented in Table 4.

Table 4. The result of solving the thermal problem of the process of hardfacing a spline

Mode	Maximum welding temperature T_{max}	T_{max} 5 seconds after welding	T_{max} 15 seconds after welding	T_{max} 25 seconds after welding	T_{max} 50 seconds after welding
1	1638°C	219°C	165°C	135°C	96°C
2	1671,1°C	257,53°C	168,41°C	141,76°C	109,05°C
3	1683°C	251,19°C	187,47°C	156,97°C	125,85°C
4	1697,3°C	312,32°C	214,2°C	164,42°C	128,71°C
5	1679,6°C	363,61°C	238,63°C	167,01°C	141,64°C

When using the Welding Distortion extension to determine the deformations created in the hardfacing, automatic import of the load from the thermal effect of the welding arc in the hardfacing the destroyed spline surface is used.

So, in the course of the study, the calculated values of the magnitude of residual deformations were obtained (Figure 7 after the multi-pass hardfacing of a destroyed slot using the example of mode 1 from Table 2).

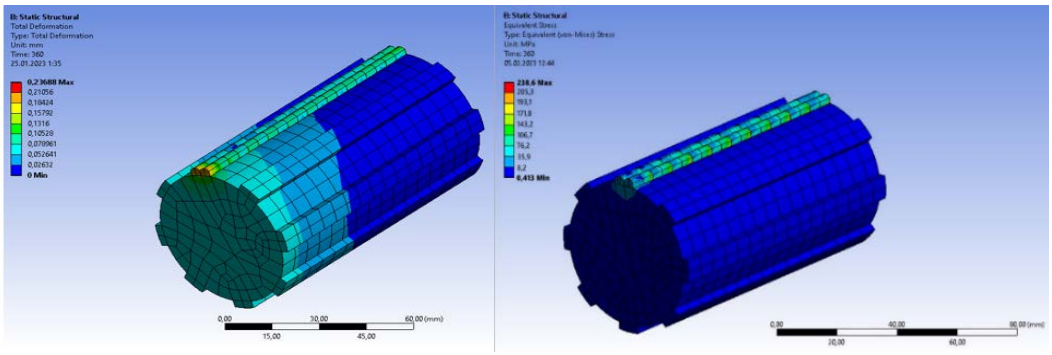

a) b)

Fig. 7. Stress-strain state of the model after surfacing of a destroyed spline: a - residual deformations of the restored spline; b - residual stresses of the restored spline

As can be seen from Figure 7a, the value of residual deformations after complete cooling of the restored spline is 0.23 mm, which is an acceptable value because deformations of the larger surface area of the spline are 0.02 mm. The value of residual stresses in the deposited layer ranges from 59.9 to 238 MPa.

The result of modeling the stress-strain state when using other hardfacing modes of the splined shaft with parameters from Table 2 is presented in Table 5.

Table 5. The result of the calculation of residual deformations of the restored spline

Mode	Residual deformations		Residual stresses	
	Max (mm)	Min (mm)	Max (MPa)	Min (MPa)
1	0,236	0,026	238,6	0,413

Mode	Residual deformations		Residual stresses	
	Max (mm)	Min (mm)	Max (MPa)	Min (MPa)
2	0,301	0,033	295,85	0,649
3	0,331	0,368	312,68	0,591
4	0,326	0,0362	310,82	0,748
5	0,391	0,0435	354,01	1,042

It can be concluded that with an increase in parameters in hardfacing modes, there is a tendency to increase residual deformations samples. To determine the similarity of the welds in the experiment and in the simulation, the appearance of the welds was compared with the transition boundary.

Figure 8 shows models of welds obtained as a result of the experiment and modeled in ANSYS Workbench with the Moving Heat Source extension. Experimental samples and simulated weld seams are made with similar mode parameters.

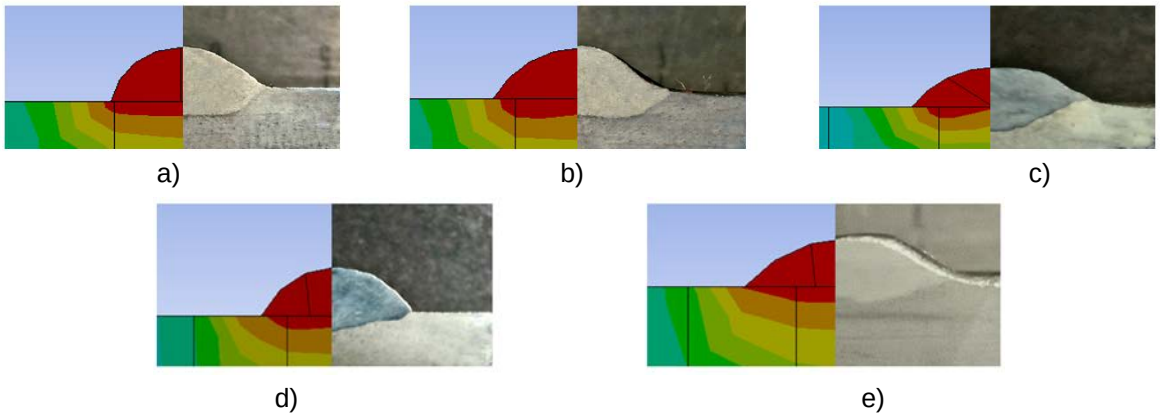

Fig. 8. Comparison of weld seams obtained by modeling and experiment: a) I=135A, U=20V; b) I=180A, U=19,5V; c) I=220A; U=20V; d) I=240A, U=22V; e) I=260A, U=22V

Analyzing the obtained structures, one can come to the conclusion about the magnitude of the temperature fields distribution in the structure of the deposited surface (Figure 9) and, consequently, obtaining the required quality of the restored shaft and the deposited weld.

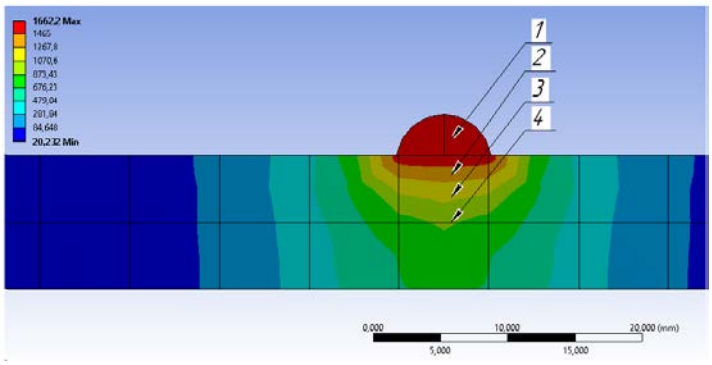

Fig. 9. Zones of temperature fields distribution in the structure of the part (on the example of mode 1: I=135A, U=20V): 1 zone - T= >1662°C; 2 zone - T= >1465°C; 3 zone - T= >873.43°C; zone 4 – T= >676.23°C

Figure 9 shows that when modeling welding, there is a penetration of the surface of the part and penetration of the weld material into the structure of the part. So zone 1 is the area of formation of the deposited weld and penetration of the deposited material into the structure of the weld (T = >1400°C). Zones 2 - 4 are zones of thermal influence on the structure of the part. Based on this, it is possible to predict the depth of penetration of the deposited weld, as well as the size of the zone of structural transformations in the body of the part. This contributes to the determination of the most optimal values of the hardfacing mode parameters.

Analyzing the data of Figures 8 and 9, we can conclude that when modeling the surfacing process, taking into account the error of the problem being solved, the simulated welds and the welds obtained experimentally are similar in terms of geometric parameters and penetration depth of the base metal. This indicates a high degree of reliability of the results and the possibility of using the selected extensions to simulate the process of hardfacing the destroyed surface of splined shafts.

4 CONCLUSIONS

1) Finite element analysis can be used to simulate the hardfacing of splined shafts and predict the optimal hardfacing parameters such as amperage and voltage.
2) Analysis of the residual temperature fields of the restored part indicates the presence of a dependence on the development of residual deformations on the selected parameters of the hardfacing mode.
3) Optimal mode of semi-automatic hardfacing: I=135A, U=20V.
4) This mode provides:
   - minimum stresses (0.413 - 238.6 MPa);
   - minimum deformations (0.026 - 0.236 mm).
5) The hardfacing process modeling method can be used for preliminary analysis of residual stresses, achievement of the desired temperature of the base metal, as well as reduction of residual stresses and deformations, which improves the quality of the obtained restored surfaces.8) The proposed computational model, based on an accurate determination of heat release, is an intermediate step towards the final goal - predicting structural changes in the heat-affected zone.

5 REFERENCES

[1] Klimpel, A. (2020). Industrial surfacing and hardfacing technology, fundamentals and applications Welding Technology Review, 91(12), 33-42, DOI: 10.26628/wtr.v91i12.1094
[2] Karasev, M., Rabotinsky, D., Kalinin, M., Potapov, N., Eremin, D. I., Lyubochko, D. (2017). Special features of seamless flux-cored wires for gas-shielded welding, Welding International, Volume 31, Issue 10, 817-822 DOI:0.1080/09507116.2017.1343983
[3] Garbade, R., Dhokey, N. (2021). Overview on Hardfacing Processes, Materials and Applications IOP Conf. Ser.: Mater. Sci. Eng., 1017, 012033, DOI 10.1088/1757-899X/1017/1/012033
[4] Waidande, S.K., Kolhe, K.P. (2017). Elementary study of submerged arc welding for hardfacing and surface engineering JETIR, Volume 4, Issue 05, 57 - 63 Paper ID:JETIR1705014
[5] Krylova S. E., Oplesnin S. P., Goltyapin M. I. (2018). Influence of gas-powder laser cladding's technological parameters on structural characteristics of corrosion-resistant steels' restored surface layer IOP Conf. Series: Materials Science and Engineering, 327, 042058 DOI:10.1088/1757-899X/327/4/042058
[6] Barka, N., Karganroudi, S., Fakir, R., Thibeault, P., Kemda V. (2020) Effects of Laser Hardening Process Parameters on Hardness Profile of 4340 Steel Spline - An Experimental Approach, Coatings, 10(4), 342; https://doi.org/10.3390/coatings10040342
[7] Tsibulskiy I. A., Somonov V. V., Korsmik R. S., Gushchina M. O., Eremeev A. D. (2018). The influence of technological parameters on the structure formation of aluminum alloys during direct deposition of wire IOP Conf. Series: Journal of Physics: Conf. Series, 1109, 012032
[8] Zhu Z., Wang, M., Zhang, H., Zhang, X., Yu, T., Wu, Z. (2017). A Finite Element Model to Simulate Defect Formation during Friction Stir Welding, Metals, 7, 256; DOI:10.3390/met7070256
[9] Puoza, J., Uba, F. (2021) Modeling and Simulation of Surfacing Welding Remanufacturing for Tunnel Boring Machine Disc Cutter, Welding International, 36(10), DOI: 10.1080/09507116.2021.1973353
[10] Kollár, D., Kövesdi, B., Néző, J. (2017). Numerical Simulation of Welding Process – Application in Buckling Analysis Periodica Polytechnica Civil Engineering, 61(1), 98–109, DOI:10.3311/PPci.9257
[11] Venkateswarlua, K., Kumar, N.P., Kumar P.S. (2018) Finite Element Simulation of Temperature Distribution, Distortion and Residual Stresses of Dissimilar Welded Joints Materials Today: Proceedings, 5, 11933–11940 DOI:10.1016/j.matpr.2018.02.167
[12] Li, W., Yu, R., Huang, D., Wu, J., Wang, Y., Hu, T., Wang, J. (2019). Numerical simulation of multi-layer rotating arc narrow gap MAG welding for medium steel plate Journal of Manufacturing Processes, Volume 45, 460-471 https://doi.org/10.1016/j.jmapro.2019.07.035
[13] Tian, L., Xing, S., Luo, G. (2022). Numerical simulation of hardfacing remanufacturing for large-scale damaged grinding roller The International Journal of Advanced Manufacturing Technology, volume 118, 1-37, 2613–2649, DOI:10.1007/s00170-021-08073-4
[14] Khudyakov, A., Korobov, Yu., Danilkin, P., Kvashnin, V. (2019). Finite element modeling of multiple electrode submerged arc welding of large diameter pipes IOP Conf. Series: Materials Science and Engineering, 681, 012025, DOI:10.1088/1757-899X/681/1/012025
[15] Choudhary T., Chaudhary K. Advanced Welding Processes: Theory and Applications (2017). – Riga: LAP LAMBERT Academic Publishing. – 116 p.
[16] Boudiaf, A., Djeghlal, L. (2018). Modeling and Numerical Simulation of Thermal Cycles During GTAW Welding SSRN Electronic Journal, 12 – 14 November, 1- 8, DOI: 10.2139/ssrn.3389786

[17] Parvez, S., Siddiqui, M., Ali, M., Dobrotă, D. (2021). Modeling of Melt Flow and Heat Transfer in Stationary Gas Tungsten Arc Welding with Vertical and Tilted Torches, Materials (Basel), 14(22), 6845, DOI: 10.3390/ma14226845

[18] Ngo, T., Toan, N., Than, V. (2018). The Simulation of welding temperature distribution, stress and distortion in GTAW process for T-joint HỘI NGHỊ KHOA HỌC VÀ CÔNG NGHỆ TOÀN QUỐC VỀ CƠ KHÍ LẦN THỨ V – VCME, 1 - 9

Paper submitted: 09.02.2023.

Paper accepted: 01.06.2023.